ELSEVIER

Journal of Molecular Structure (Theochem) 594 (2002) 199–206

THEO CHEM

www.elsevier.com/locate/theochem

Further studies on the rotational barriers of Carbamates. An NMR and DFT analysis of the solvent effect for Cyclohexyl *N*,*N*-dimethylcarbamate

Ernani A. Basso*, Rodrigo M. Pontes

Departamento de Quimica, Universidade Estadual de Maringa, Av. Colombo 5790, 87020-900 Maringá, Paraná, Brazil

Received 7 April 2002; accepted 26 June 2002

Abstract

The solvent effect on the Gibbs energy of activation for rotation around the (C=O)–N bond in cyclohexyl *N*,*N*-dimethylcarbamate was investigated by dynamic NMR spectroscopy and density-functional theory at the B3LYP/6-311 + G** level. The experimental barriers were about 15 kcal mol^{-1} with no appreciable variation when the solvent polarity was changed. A reaction field model was applied to theoretically mediate the solvent effect and the results were comparable to the experimental data. An analysis, based on the Onsager solvation theory, showed that the solvent effect on rotational barriers can be understood employing the total molecular dipole moment, the difference between the dipole moments of the ground and the transition state structures, or both, as appropriate.

Keywords: Carbamates; Rotational barriers; DFT calculations; SCRF theory

1. Introduction

The barrier to rotation around conjugated C–N bonds has been the subject of substantial investigation [1–11]. The efforts to understand and theoretically quantify rotational barriers have enriched our understanding about the electronic structure of molecules. In this respect, amides are the most studied systems, characterized by their high barrier to rotation about the (C=O)–N bond (15–20 kcal mol^{-1} typically); their planarity and their low susceptibility to nucleophilic attack at the carbonyl carbon. The most used explanation for these properties employs the resonance model, although some authors have criticized this interpretation [6,7].

Measurements by NMR spectroscopy, both in the gas phase and in solution, have shown that the rotational barrier in amides is remarkably affected by the solvent medium [9–11,16]. Even though satisfactory agreements between experiment and theoretical calculations were obtained for the gas phase, there were also efforts to reproduce the behavior in solution [11,16]. For this purpose, the reaction field theory, implemented in molecular orbital calculations as self-consistent reaction field (SCRF) theory [12–15], has been a suitable tool, delivering excellent results for solvents which have no specific interactions, such as hydrogen bonding [16–18]. For solvents like water, the inclusion of some or even just one solvent

* Corresponding author. Tel.: +55-44-261-4332; fax: +55-44-263-5784.

E-mail address: eabasso@uem.br (E.A. Basso).

0166-1280/02/$ - see front matter
PII: S0166-1280(02)00391-3

molecule in strategic positions around the solute has been an efficient approach [16,19].

However, the powerful of SCRF theory goes beyond to simply reproduce the experimental results, but rather it can be used to answer questions that are not accessible to experiments. For instance, the rotational barrier in *N*,*N*-dimethylacetamide (DMA) was found to be somewhat more solvent sensitive than in *N*,*N*-dimethylformamide (DMF) [16]. In the former, the barrier increases by 2.44 kcal mol^{-1} on going from the gas phase to acetonitrile solution, whereas in DMF the increase in only 1.38 kcal mol^{-1}. This result has been explained in terms of the difference between the dipole moments of the ground state (GSs, Fig. 1) and the lower energy transition state structure (TS1s or TS2s, Fig. 1). TS2 is preferred in polar solvents for DMF, while TS1 is the favored path for DMA. Once the dipole moment of TS2 is much closer to that of the GS structure, the solvent effect on the rotational barrier in DMF must be determined by a small difference in dipole moments, while in DMA a large difference is predominant. Hence, the destabilization of the transition state structure compared with the ground state structure is expressively stronger in DMA.

Carbamates share the same structural features of amides, having an –OR group replacing the hydrogen or alkyl substituent attached to the carbonyl carbon. Nevertheless, a different behavior is observed in solution for that system. It has been found that, for a series of simple carbamates, the rotational barrier is apparently insensitive to the solvent polarity [20]. Theoretical calculations has shown that the difference in the dipole moments of GS and TS is similar for amides and carbamates, and a similar response should be expected for both systems [18]. The lower total molecular dipole moment of carbamates relative to amides was pointed out as the main factor for the insensitivity of their rotational barrier.

In this work, we are interested in assessing the current proposals used to explain the solvent effect on the rotational barrier in carbamates and amides. For this purpose, we have performed density-functional theory (DFT) and SCRF calculations for DMF and cyclohexyl *N*,*N*-dimethylcarbamate (CDMC), along with dynamic NMR measurements for the latter, which has no experimental data available.

2. Experimental

2.1. Materials

Cyclohexyl *N*,*N*-dimethylcarbamate was obtained from the reaction of *N*,*N*-dimethylcarbamyl chloride with sodium-treated cyclohexanol in tetrahydrofuran; bp 88–90 °C/0.7 Torr [21].

Deuterated solvents were obtained commercially and used as received. Carbon disulfide was distilled and stored over molecular sieves prior to use.

2.2. NMR experiments

NMR spectra were acquired on a Varian Gemini-2000/300 spectrometer (300 MHz for ^{1}H and 75.5 MHz for ^{13}C). Samples were prepared by placing 50 mg of the compound in 0.5 ml of the appropriate solvent in a 5 mm NMR tube. For CS_2, $(CD_3)_2CO$ was used as external reference. ^{13}C spectra were obtained with sweep widths ranging from 12.5 to 16.5 kHz, a 30° flip angle (pulse width of 6.5 μs), 128–256 scans with a delay time of 1 s, and stored in a 16 K data block.

The variable temperature probe was calibrated against vacuum-sealed methanol and ethylene glycol standards. For each solvent, spectra at several temperatures were acquired in order to determine the maximum separation between the signals of the exchanging nucleus ($\Delta\nu$) and the coalescence temperature (T_c). Gibbs energies of activation at the coalescence temperature ($\Delta G_c^{\ddagger}$) were calculated using the Eyring's equation,

$$\Delta G_c^{\ddagger} = 4.58 T_c[10.32 + \log(T_c/k_c)] \quad (1)$$

where $k_c(= \pi\Delta\nu/2^{1/2})$ is the rate constant for the exchange process at T_c [22,23].

2.3. Calculations

The GAUSSIAN 98 package [24] was used to carry out all the calculations. DFT was applied with the Becke's 3-parameter hybrid method [25] and correlation functional of Lee, Yang and Parr (B3LYP) [26], in conjunction with the 6-311 + G^{**} basis set.

Ground state structures were optimized in the gas phase and in solution utilizing the Onsager model [12]

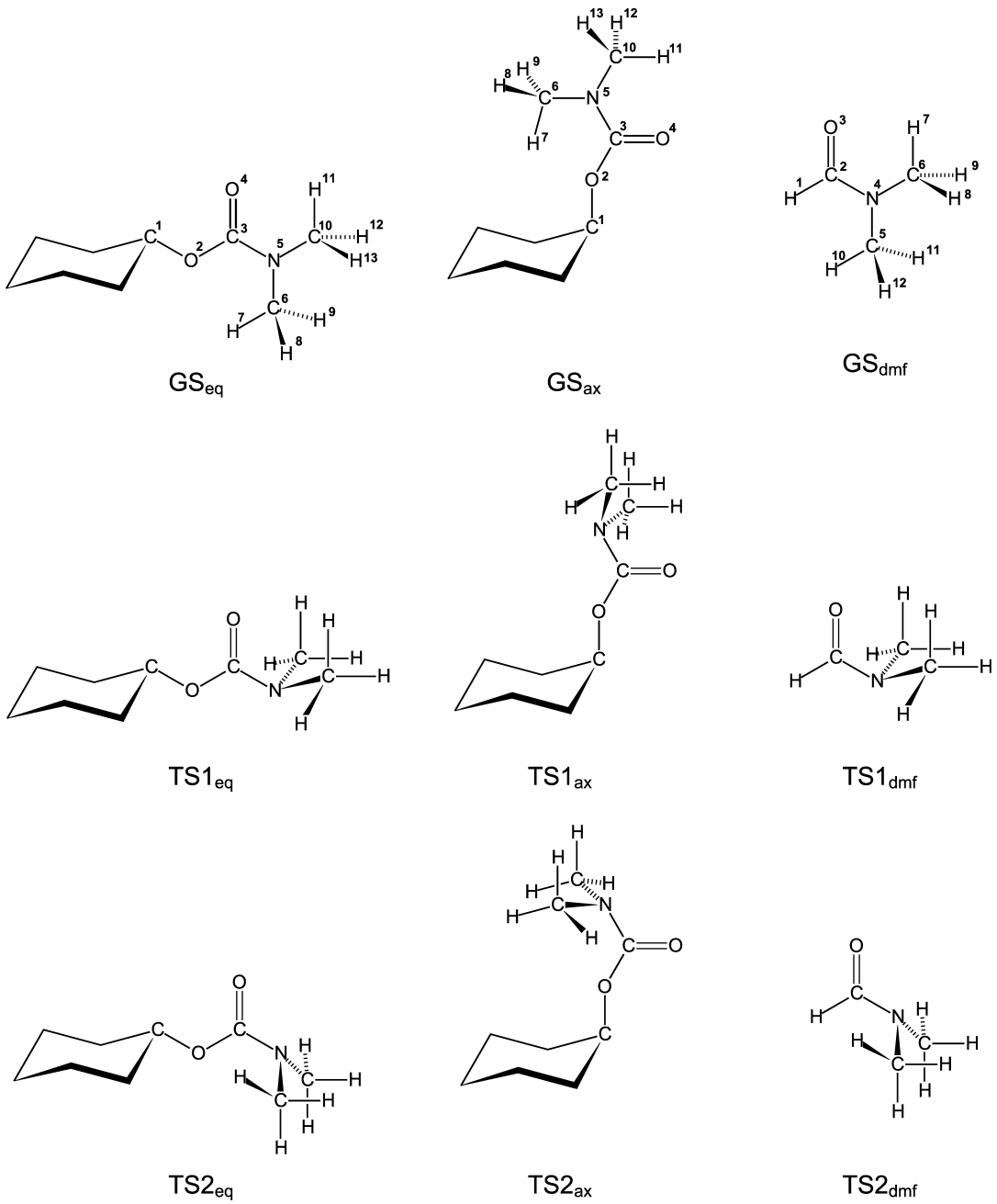

Fig. 1. Molecular structures and atom numbering for the studied compounds.

and SCRF protocol [14]. The synchronous transit-guided quasi-Newton (STQN) method [27,28], invoked by the QST3 option, was used to locate transition structures. This procedure requires the specification of products, reagents and an initial guess for the transition state. To get a first approximation to the latter, we have performed an AM1 relaxed potential-energy surface calculation by varying the ϕ(O2–C3–N5–C10) angle for CDMC and the ϕ(O3–C2–N4–C5) angle for DMF, with increments

of 10°. A molecular volume calculation was performed over the gas-phase structures prior the SCRF routines. Stationary points were assigned as minima or saddle points by frequency calculations and a 0.9806 scale factor was used for zero-point energy corrections [29].

3. Results and discussion

Tables 1 and 2 present the calculated geometries for CDMC and DMF, respectively. Table 3 lists the energies and dipoles for the species of Fig. 1. Herein, we are going to discuss the results of SCRF–DFT calculations.

3.1. Experimental and calculated Gibbs energies of activation

In Table 4 we present the results of the dynamic NMR experiments for CDMC. Those values actually correspond to a weighted average between that of the equatorial and the axial conformers. To take this fact into account in our theoretical estimates, we have calculated the conformer populations for each solvent (Table 5). For comparison, our gas-phase result for the equatorial conformer population, viz. 82.91%, is in good agreement with an early determination by NMR spectroscopy ($82 \pm 2\%$ in 10% CD_2Cl_2/CF_2Br_2) [21]. The final $\Delta G^{\ddagger}$ values were calculated from

Table 1
Selected structural parameters in the gas phase for cyclohexyl *N*,*N*-dimethylcarbamate (bond lengths in Å, bond angles in degrees)

Parameter	Species					
	GS_{eq}	$TS1_{eq}$	$TS2_{eq}$	GS_{ax}	$TS1_{ax}$	$TS2_{ax}$
Bond lengths						
r(C1–O2)	1.453	1.460	1.459	1.460	1.467	1.466
r(O2–C3)	1.360	1.338	1.352	1.360	1.338	1.351
r(C3–O4)	1.218	1.209	1.203	1.218	1.209	1.203
r(C3–N5)	1.370	1.433	1.428	1.367	1.433	1.429
r(N5–C6)	1.456	1.468	1.466	1.456	1.468	1.465
r(N5–C10)	1.455	1.468	1.466	1.455	1.468	1.466
r(C6–H7)	1.086	1.100	1.092	1.085	1.100	1.092
r(C6–H8)	1.098	1.092	1.093	1.098	1.092	1.100
r(C6–H9)	1.094	1.092	1.100	1.097	1.092	1.093
r(C10–H11)	1.087	1.100	1.092	1.087	1.100	1.092
r(C10–H12)	1.095	1.092	1.100	1.097	1.092	1.093
r(C10–H13)	1.097	1.092	1.093	1.095	1.092	1.100
Bond angles						
∠(C1–O2–C3)	117.0	117.7	118.1	116.8	117.6	118.0
∠(O2–C3–O4)	123.7	124.6	124.0	123.6	124.6	124.1
∠(O2–C3–N5)	111.7	110.2	111.8	111.8	110.2	111.8
∠(O4–C3–N5)	124.6	125.3	124.2	124.6	125.2	124.1
∠(C3–N5–C6)	123.9	110.9	112.7	124.2	110.8	113.0
∠(C3–N5–C10)	118.7	110.8	112.9	119.0	110.8	112.8
Dihedral angles						
ϕ(C1–O2–C3–O4)	2.7	0.2	0.4	0.9	0.1	0.9
ϕ(O4–C3–N5–C10)	5.7	62.0	115.6	3.8	63.2	114.1
ϕ(O4–C3–N5–C6)	174.7	63.2	114.9	177.8	61.7	116.5
ϕ(O2–C3–N5–C6)	−5.6	117.2	64.8	2.8	118.0	64.0
ϕ(O2–C3–N5–C10)	174.6	117.7	64.7	3.8	117.1	114.1
ϕ(C3–N5–C10–H11)	−12.8	56.5	51.2	6.1	64.7	51.1
ϕ(C3–N5–C6–H7)	20.8	61.5	51.3	14.0	64.6	51.7

Computed at the B3LYP/6-311 + G^{**} level. For definitions of the species see Fig. 1.

Table 2
Selected structural parameters in the gas phase for *N*,*N*-dimethylformamide (bond lengths in Å and bond angles in degrees)

Parameter	Species		
	GS_{dmf}	$TS1_{dmf}$	$TS2_{dmf}$
Bond lengths			
r(H1–C2)	1.105	1.105	1.117
r(C2–O3)	1.217	1.201	1.196
r(C3–N4)	1.363	1.441	1.435
r(N4–C5)	1.451	1.471	1.468
r(N4–C6)	1.455	1.471	1.468
r(C6–H7)	1.088	1.093	1.091
r(C6–H8)	1.095	1.092	1.092
r(C6–H9)	1.095	1.099	1.104
r(C5–H10)	1.091	1.093	1.091
r(C5–H12)	1.096	1.092	1.092
r(C5–H12)	1.096	1.099	1.104
Bond angles			
∠(H1–C2–O3)	122.2	121.3	121.0
∠(H1–C2–N4)	112.0	113.5	114.4
∠(C2–N4–C5)	121.7	111.2	109.7
∠(C2–N4–C6)	120.5	111.2	109.7
Dihedral angles			
ϕ(C2–N4–C5–H10)	0.0	55.4	60.4
ϕ(C2–N4–C6–H7)	0.0	55.5	60.5
ϕ(O3–C2–N4–C6)	0.0	62.8	118.5
ϕ(O3–C2–N4–C5)	180.0	62.8	118.4

Computed at the B3LYP/6-311 + G^{**} level. For definitions of the species see Fig. 1.

the equation:

$$\Delta G^{\ddagger} = n_{eq}\Delta G^{\ddagger}_{eff,eq} + n_{ax}\Delta G^{\ddagger}_{eff,ax} \quad (2)$$

where n_{eq} and n_{ax} refer to the population of the equatorial and the axial conformer, respectively; $\Delta G^{\ddagger}_{eff,eq}$ and $\Delta G^{\ddagger}_{eff,ax}$ refer to the effective Gibbs energies of activation in which the contribution of TS1 and TS2 has been taken into account. Table 6 lists the final estimates for $\Delta G^{\ddagger}$.

Reaction field theory, used here to mediate the solvent effect, has been successfully applied to isomerization processes. The simplest approach, due to Kirkwood and Onsager [12,13], is based on the interaction of the solute's dipole moment with the bulk solvent. The dipole induces an electric field in the solvent, which in turn interact with the solute dipole leading to stabilization. The solute is placed in a spherical cavity, which is a good approximation for small molecules, but can lead to nonrealistic results

Table 3
Gas-phase energies (in hartrees), zero-point corrections (in kcal mol^{-1}) and dipole moments (in debyes) for cyclohexyl *N*,*N*-dimethylcarbamate and *N*,*N*-dimethylformamide

Species	Energy	Zero-point correction	Dipole moment
GS_{eq}	−558.590072	158.38	2.34
$TS1_{eq}$	−558.565670	158.17	1.24
$TS2_{eq}$	−558.564407	157.87	3.04
GS_{ax}	−558.588614	158.40	2.50
$TS1_{ax}$	−558.564668	158.31	1.24
$TS2_{ax}$	−558.563045	158.05	3.09
GS_{dmf}	−248.590164	62.64	4.24
$TS1_{dmf}$	−248.554380	61.85	1.92
$TS2_{dmf}$	−248.554815	61.67	3.49

Computed at the B3LYP/6-311 + G^{**} with ZPE correction scaled by 0.9806. For definitions of the species see Fig. 1.

for the larger ones. In a spherical cavity, there would be regions in which the charge distribution of the solute should be closer to the boundaries than in the others, giving rise to nonphysical interactions [15]. Such problem can lead to large errors in the absolute energy. However, in intramolecular isomerization processes these kinds of interaction do not change too much on going from reagents to products, and a cancellation of errors usually produces values comparable to the experimental data. The results in Table 6, computed with the above theory, have a very good agreement with the NMR measurements.

We have also performed calculations for DMF. This compound has been studied before in a number of works [3–8], but not at the same level of theory used in this work for CDMC. The calculated $\Delta G^{\ddagger}$

Table 4
Rotational barriers for cyclohexyl *N*,*N*-dimethylcarbamate measured by dynamic NMR ^{13}C experiments (T_c in K, $\Delta\nu$ in Hz, and $\Delta G^{\ddagger}_c$ in kcal mol^{-1})

Solvent	T_c	$\Delta\nu$	$\Delta G^{\ddagger a}_c$
CS_2	309	34.32	15.5
$CDCl_3$	304	30.35	15.3
CD_2Cl_2	304	27.83	15.3
$(CD_3)_2CO$	302	27.44	15.2
CD_3CN	300	24.27	15.2
10% D_2O/CD_3OD	302	24.83	15.3

Measurements perfomed at 75.5 MHz.
[a] Values estimated to be within ± 0.2 kcal mol^{-1}.

Table 5
Calculated equatorial conformer populations for cyclohexyl *N,N*-dimethylcarbamate

Solvent	ϵ	% eq
Gas phase	1.0	82.91
Carbon dissulfide	2.6	81.64
Chloroform	4.9	80.77
Dichloromethane	8.9	80.37
Acetone	20.7	79.77
Acetonitrile	36.6	79.56

Computed at the B3LYP/6-311 + G** with ZPE correction scaled by 0.9806.

values for DMF, Table 7, are slightly overestimated when compared to the experimental data of Ref. [16]. However, the trend of the outcomes is well reproduced and, to the current purposes, the results derived from the B3LYP/6-311 + G** level will suffice.

3.2. Solvent effect on the rotational barrier

The difference in dipole moments of GS and TS structures was used before to explain the solvent effect on the rotational barrier in amides [16,10]. The GS_{dmf} structure has a dipole moment higher than both $TS1_{dmf}$ and $TS2_{dmf}$ (Table 3), and it must be relatively stabilized when the solvent polarity increases. The greater the difference between the dipole moments of GS and TS structures, the greater should be the

Table 6
Calculated Gibbs energies of activation (in kcal mol^{-1}) for cyclohexyl *N,N*-dimethylcarbamate

ϵ	$TS1_{eq}$	$TS2_{eq}$	$TS1_{ax}$	$TS2_{ax}$	eff. eq[a]	eff. ax[a]	av[b]
1.0	15.11	15.59	14.94	15.69	14.89	14.79	14.87
2.6	15.26	15.64	15.14	15.54	15.01	14.90	14.99
4.9	15.33	15.56	15.22	15.46	15.02	14.92	15.00
8.9	15.38	15.51	15.28	15.41	15.03	14.93	15.01
20.7	15.41	15.47	15.34	15.37	15.03	14.94	15.01
36.6	15.42	15.45	15.35	15.36	15.02	14.94	15.00

Computed at the B3LYP/6-311 + G** level with ZPE correction scaled by 0.9806. For definitions of the species see Fig. 1.
[a] Effective barrier, incorporanting the contribution of both transition states.
[b] Averaged barrier, taking into account the populations of equatorial and axial conformers.

Table 7
Calculated Gibbs energies of activation (kcal mol^{-1}) for *N,N*-dimethylformamide in solution (kcal mol^{-1})

ϵ	TS1[a]	TS2[a]	Effective[a]	Exp.[b]
1.0	21.66	21.21	20.98	19.25
2.6	22.64	21.55	21.47	–
4.9	23.10	21.72	21.66	–
8.9	23.38	21.82	21.78	–
20.7	23.60	21.90	21.87	20.45
36.6	23.68	21.93	21.90	20.65

Computed at the B3LYP/6-311 + G** with ZPE scaled by 0.9806. For definitions of the species see Fig. 1.
[a] Effective barrier, incorporating the contribution of both transition states.
[b] Values from Ref. [16].

variation in the rotational barrier for a given compound. This is well illustrated by DMF and DMA as aforementioned, but an interesting situation arises when we compare amides and carbamates.

Take, for instance, the preferred transition state for DMF ($TS2_{dmf}$) and which one of the transition states for equatorial CDMC ($TS1_{eq}$ or $TS2_{eq}$). In the gas phase, $TS2_{dmf}$ has a dipole moment 0.75 D lower than that of GS_{dmf}, while for CDMC the dipole moment of the $TS2_{eq}$ structure is 1.10 D higher than that of GS_{eq} (Table 3). According to these data, an even strong dependence with the solvent polarity should be expected for the carbamate, but the barrier for CDMC via $TS2_{eq}$ decreases only 0.14 kcal mol^{-1}, whereas for DMF an increase of 0.72 kcal mol^{-1} was obtained on going from the gas phase to acetonitrile solution (Tables 6 and 7). To overcome this problem, it has been proposed that the total dipole moment of the species should be considered [18]. Actually, the Onsager's equation predicts a quadratic dependence on the dipole moment for the electrostatic solvation free energy [12] and the solvent effect on rotational barriers should also follow a quadratic profile. Since the amides' dipole moments are typically twice that of carbamates, the rotational barrier in the former must be more solvent sensitive, even with similar differences between the dipole moments of GS and TS.

However, calculations at the MP2(fc)/6-31 + G* level showed that the dipole moment of DMF is a little higher than that of DMA, and a prediction based on the total molecular dipole moment gives the opposite

result as compared to the experimental data [16]. For this reason, we have examined closely the parameters employed in comparing the solvent effect for different compounds. In this way, consider the Onsager's equation,

$$\Delta G_{\text{solv}} = -(\epsilon - 1)\mu^2/(2\epsilon + 1)a_0^3 \quad (3)$$

where μ is the solute dipole moment, ϵ is the dielectric constant of the medium, and a_0 is the radius of the cavity where the solute is situated [12]. Suppose that a_0 has the same value for GS and TS, which is a reasonable approximation for simple compounds, and let us write the TS dipole as $\mu_{\text{TS}} = \mu_{\text{GS}} + \delta\mu$; $\delta\mu$ being the difference between the dipoles for GS and TS ($\mu_{\text{TS}} - \mu_{\text{GS}}$). Substitution of this result into Eq. (3) gives the following expression for the solvation energy of TS:

$$\Delta G_{\text{solv}}^{\text{TS}} = -\xi(\epsilon, a_0)\mu_{\text{GS}}^2 - 2\xi(\epsilon, a_0)\mu_{\text{GS}}\delta\mu - \xi(\epsilon, a_0)\delta\mu^2 \quad (4)$$

where

$$\xi(\epsilon, a_0) = (\epsilon - 1)/(2\epsilon + 1)a_0^3$$

Now, the first term in Eq. (4) is just the solvation energy for GS in a medium of dielectric constant ϵ. The remaining terms express how differently GS and TS are affected by the solvent polarity.

Consider two systems, which have similar dipoles for the GSs. The first term in Eq. (4) will be similar for both, and the difference in the observed behavior for each system will be determined by $\delta\mu$. The DMF and DMA case, mentioned above, matches this situation. However, when we deal with systems with dipole moments remarkably different for the GSs, the first term in Eq. (4) must be used to compare their behavior. The latter approach is recommended for comparing amides and carbamates, and correctly predicts a solvent effect much more pronounced for an amide. Of course, between these extreme cases there would be intermediary situations, for which μ as well as $\delta\mu$ should be considered.

Finally, an additional factor must contribute to the insensitivity of the rotational barrier to the bulk solvent polarity in CDMC and other carbamates. In DMF, as an example, both TS have a dipole moment lower than GS, while in CDMC the TS2 s have larger dipole moments compared with the GSs (Table 3). Hence, the rotational barrier must decrease for the isomerization via TS2 for CDMC, and increase via TS1. Nevertheless, the observed rotational barrier must reflect the behavior for both TS, i.e. the increase in the reaction rate through one path is compensated by the decrease through the other path.

4. Summary

The rotational barrier for CDMC was studied by NMR spectroscopy and SCRF–DFT theory, and an excellent agreement was obtained between them. Bulk solvent polarity has little or practically no effect on the rotational barrier of this carbamate, in agreement with earlier reports for similar compounds. An analysis based on the Onsager's equation for the solvation energy was satisfactory. The total molecular dipole moment is appropriate for predicting the solvent effect on the rotational barrier for a given compound. However, when comparing the behavior of different compounds, either the total molecular dipole moment or the difference between the dipole moments of the ground state structure and the transition state structure must be employed, according the values of the dipoles for the ground state structures. Intermediary situations require both quantities usage. This approach seems to be suitable for a qualitative understanding of the solvent effect on the kinetics of rotational isomerism.

Acknowledgments

We acknowledge to CENAPAD-SP for computer facilities and Fundação Araucária, and FAPESP, for financial support for this research. A scholarship from CAPES (to R.M.P) is also acknowledged.

References

[1] W.E. Stewart, T.H. Siddal III, Chem. Rev. 70 (1970) 517.
[2] B.D. Ross, N.S. True, J. Am. Chem. Soc. 106 (1984) 2451.
[3] K. Lim, M.M. Francl, J. Phys. Chem. 91 (1987) 2716.
[4] K.B. Wiberg, P.R. Rablen, J. Am. Chem. Soc. 114 (1992) 831.
[5] K.B. Wiberg, L.M. Cameron, J. Am. Chem. Soc. 115 (1993) 9234.

[6] K.E. Laidig, L.M. Cameron, J. Am. Chem. Soc. 118 (1996) 1737.
[7] D. Lauvergnat, P.C. Hiberty, J. Am. Chem. Soc. 119 (1997) 9478.
[8] N.G. Vassilev, V.S. Dimitrov, J. Mol. Struct. 484 (1999) 39.
[9] T. Drakenberg, K.J. Dahlquist, J. Forsen, J. Phys. Chem. 76 (1972) 2178.
[10] C.B. LeMaster, N.S. True, J. Phys. Chem. 93 (1989) 1307.
[11] E.M. Duffi, D.L. Severance, W.L. Jorgensen, J. Am. Chem. Soc. 114 (1992) 7235.
[12] L. Onsager, J. Am. Chem. Soc. 58 (1936) 1486.
[13] J.G. Kirkwood, J. Chem. Phys. 2 (1934) 351.
[14] M.W. Wong, K.B. Wiberg, M. Frish, J. Phys. Chem. 95 (1991) 8491.
[15] J. Tomasi, M. Persico, Chem. Rev. 94 (1994) 2027.
[16] K.B. Wiberg, P.R. Rablen, D.J. Rush, T.A. Keith, J. Am. Chem. Soc. 117 (1995) 4261.
[17] P.R. Rablen, D.A. Miller, V.R. Bullock, P.H. Hutchinson, J.A. Gorman, J. Am. Chem. Soc. 121 (1999) 218.
[18] P.R. Rablen, J. Org. Chem. 65 (2000) 7930.
[19] J.R. Pliego, J.M. Riveros, J. Phys. Chem. A 30 (2001) 7241.
[20] C. Cox, T. Lectka, J. Org. Chem. 63 (1998) 2426.
[21] E.A. Basso, P.R. Oliveira, J. Caetano, I.T.A. Schuquel, J. Braz. Chem. Soc. 12 (2001) 215.
[22] J.F. Kincaid, H. Eyring, A.E. Stearn, Chem. Rev. 28 (1941) 301.
[23] A. Allerhand, H.S. Gutowsky, J. Jonas, R.A. Meinzer, J. Am. Chem. Soc. 88 (1966) 3185.
[24] M.J. Frisch, G.W. Trucks, H.B. Schlegel, G.E. Scuseria, M.A. Robb, J.R. Cheeseman, V.G. Zakrzewski, J.A. Montgomery, Jr., R.E. Stratmann, J.C. Burant, S. Dapprich, J.M. Millam, A.D. Daniels, K.N. Kudin, M.C. Strain, O. Farkas, J. Tomasi, V. Barone, M. Cossi, R. Cammi, B. Mennucci, C. Pomelli, C. Adamo, S. Clifford, J. Ochterski, G.A. Petersson, P.Y. Ayala, Q. Cui, K. Morokuma, D.K. Malick, A.D. Rabuck, K. Raghavachari, J.B. Foresman, J. Cioslowski, J.V. Ortiz, A.G. Baboul, B.B. Stefanov, G. Liu, A. Liashenko, P. Piskorz, I. Komaromi, R. Gomperts, R.L. Martin, D.J. Fox, T. Keith, M.A. Al-Laham, C.Y. Peng, A. Nanayakkara, M. Challacombe, P.M.W. Gill, B. Johnson, W. Chen, M.W. Wong, J.L. Andres, C. Gonzalez, M. Head-Gordon, E.S. Replogle, J.A. Pople, GAUSSIAN 98 (Revision A.9), Gaussian Inc., Pittsburgh PA, 1998.
[25] A.D. Becke, J. Chem. Phys. 98 (1993) 1372.
[26] C. Lee, W. Yang, R.G. Parr, Phys. Rev. B 37 (1988) 785.
[27] C. Peng, P.Y. Ayala, H.B. Schlegel, M.J. Frisch, J. Comput. Chem. 17 (1996) 49.
[28] C. Peng, H.B. Schlegel, Isr. J. Chem. 33 (1994) 449.
[29] A.P. Scott, L. Radon, J. Phys. Chem. 100 (1996) 16502.